Journal of Materials Chemistry

Cite this: J. Mater. Chem., 2011, 21, 10823

www.rsc.org/materials

PAPER

Whispering gallery mode emission generated in tunable quantum dot doped glycerol/water and ionic liquid/water microdroplets formed on a superhydrophobic coating†

Edin Nuhiji,*[a] François G. Amar,*[b] Hongxia Wang,[a] Nolene Byrne,[a] Tich-Lam Nguyen[c] and Tong Lin[a]

Received 4th February 2011, Accepted 5th May 2011
DOI: 10.1039/c1jm10531k

Emission spectra from microdroplets doped with CdSe/ZnS quantum dots (QDs) have been recorded on superhydrophobic coatings (water contact angle > 170°). Whispering gallery modes (WGMs) with *Q*-factors as high as 4.0×10^3 were discernible. Excitation parameters for optimal microdroplet WGM response illumination and acquisition are also presented. Fluorescent QDs provide a robust WGM reporting mechanism under extreme continuous wave microdroplet excitation (465.5 μW) for periods greater than 15 minutes. In this format droplets could be optically tuned on demand using combinations of QDs. Ionic liquid QD-doped droplet emission was found to be spectrally stable: a >75% improvement in WGM blue-shift was recorded (due to droplet evaporation) compared to QD-doped glycerol/water droplet emission. Theoretical analysis of emission spectra confirmed the observed emission response curves correspond to Mie theory suggesting the droplets are extremely close to spherical on the surface. This versatile liquid resonator system has direct implications in high performance room-temperature laser development, telecommunications research and lab-on-a-chip based diagnostics.

Introduction

Optical whispering gallery mode (WGM) resonators have received significant attention in recent years because of their potential applications in optic fibre technology, telecommunication[1] and biosensor systems.[2]

Characteristically the circular optical modes or WGM observed in the resonator are produced by an optical confinement effect created by the resonator's high-refractive-index contrast with the external medium.[3–5]

Under these conditions a light-wave that preferentially couples into the resonator is trapped and then totally internally reflected through the inner volume. The unique intensity pattern (WGM profile) and quality (*Q*-factor) of the response are precisely defined by the diameter, refractive index and surface homogeneity at the resonator/medium interface. While WGMs can be generated within various confinement geometries,[4] this investigation focuses solely on WGMs generated in spherical resonators.

In principle, microdroplets provide an extremely powerful and expandable platform to rapidly investigate reaction kinetics in micro- to nanolitre volumes for a range of chemical and biochemical systems.[6–10] The simple particle geometry, extremely low surface roughness and simple optical tuning based on droplet composition make microdroplets excellent WGM resonators particularly when doped with a fluorophore.[11,12] An advantage of microdroplets for chemical assays is that they can be deposited at high speed using current printer technology, facilitating high throughput of samples. Methods used to fabricate microdroplets have included dynamic levitation[13] and depositing an emulsion onto a superhydrophobic surface.[14,15] The simplest approach to "readout" of the WGM spectrum is to dope the droplet with a fluorophore, such as a commercial dye. However, organic dyes generally exhibit broad absorption/emission profiles, suffer from a low bleaching threshold, and are susceptible to chemical, thermal and photo-degradation. Such photophysical properties have limited their effectiveness in real-time or long-term fluorescence studies.[16]

Alternatives to dyes are semiconductor nanocrystals or quantum dots (QDs). Inorganic QD nanoparticles exhibit much higher fluorescence stability than organic dyes.[17,18] A typical photoluminescence half-life of CdSe core QDs is 10 ns, while the photoluminescence lifetime of CdSe/ZnS core/shell QDs is

[a]*Centre for Material and Fibre Innovation, Institute for Technology Research and Innovation, Deakin University, Geelong, Victoria, Australia 3217. E-mail: edin.nuhiji@deakin.edu.au; Fax: +61 3 5227 1103; Tel: +61 3 5227 2913*
[b]*Department of Chemistry, The University of Maine, Orono, Maine, USA 04469-5706. E-mail: amar@maine.edu; Fax: +1 207 581-1191; Tel: +1 207 581-1196*
[c]*Bio21 Institute and School of Chemistry, The University of Melbourne, Parkville, Victoria, 3010, Australia*

† Electronic supplementary information (ESI) available: Time dependent WGM emission analysis of glycerol/water and ionic liquid/water microdroplets. See DOI: 10.1039/c1jm10531k

typically between 30 and 40 ns at room temperature. QDs have a large absorption cross-section and quantum yields of up to 80% have been reported.[19–21] In addition, QDs with various emission profiles can be easily synthesized by controlling the particle size, also QD–QD pair constructs do not exhibit FRET.[22] These fluorescent properties make QDs robust alternatives to dyes for fluorescence based WGM reporting systems.[23,24] Recently QDs were successfully utilized to report WGM emission in a dynamically levitated droplet, however the system could only accommodate a single microdroplet.[25]

In this paper we demonstrate that close to spherical microdroplets can be easily prepared on very hydrophobic surfaces. These droplets exhibit stable WGMs for at least 15 minutes. We also describe for the first time the use of an ionic liquid WGM resonator, which minimizes issues of droplet evaporation. Spectra collected from excited microdroplets may contain more than 60 discernible fluorescent modes with Q values of 4.0×10^3. Superhydrophobic coatings ensure the droplet is close to spherical, which facilitates fitting of the WGM spectra to light scattering theory.

Materials and methods

Materials

Cover slips (24 × 50 mm) were purchased from ESCO, Biolab Scientific, Australia. Glycerol (n 1.47) was purchased from Ajax Finechem, Australia and Milli-Q grade (R > 18 M Ω cm) water was used throughout. An atomizer was acquired from The Perfume Connection, Australia. CdSe/ZnS core/shell QD nanocrystals were synthesized following methods reported by van Embden and Jasieniak *et al.*,[26–28] and they were phase-transferred into water using an amphiphilic polymer as prescribed by Lees and co-workers.[29] Green, yellow, orange and red emitting CdSe/ZnS QDs utilized in the experiments described in this exhibited emission maxima at λ_{max} 522 nm (green); λ_{max} 572 nm (yellow); λ_{max} 615 nm (orange); λ_{max} 622 and 631 nm (red). Aliquots of QDs were taken from a 10 μM stock solution. Anhydrous trifluoromethanesulfonic acid was purchased from Fluka and triethylamine was purchased from Sigma Aldrich; both were used as received.

Instrumentation

WGM acquisition set-up. Droplet imaging was carried out with a FV-500 Olympus Fluoview laser Scanning Microscope IX71 (Olympus, USA). Emission spectra were collected with a Triax 550 imaging spectrograph equipped with a liquid nitrogen cooled (137 K) CCD (Jobin Yvon, USA). Microdroplets were resolved and excited in the upright geometry, through an Olympus UPlanSApo 100XO objective, N.A. 1.4, working distance 0.13 mm (Scheme 1) using an 80 μm pinhole. Particles were excited with a focused laser beam 488 nm (Melles Griot, USA). The incident power was typically 465.5 μW. Emission signals were typically collected with the wavelength centre point at 600 nm (depending on the QD emission profile) through a 515 nm cut-off filter with a 2 s integration time.

Scanning electron microscopy. Scanning electron microscopy analyzed substrates were first coated with a conductive layer of gold using a gold sputter coater. Images were then collected with a Supra 55 VP, with a beam voltage of 15 keV under high vacuum (Carl Zeiss, Germany).

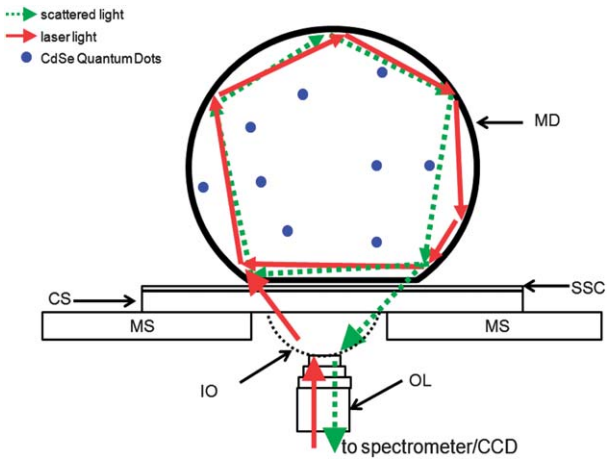

Scheme 1 Microdroplet WGM acquisition set-up. A confocal system was used to examine single microdroplets formed on the superhydrophobic surface. The WGM response was recorded with a Triax 550 spectrometer (0.05 nm spectral resolution) and a LN2CCD. In an actual single field of view 10–30 microdroplets could be identified. IO = immersion oil; SSC = superhydrophobic surface coating; CG = cover-glass; MD = microdroplet; MS = microscope stage; MO = microscope objective (Olympus UPlanSApo 100 XO).

Methods

(a) Preparation of superhydrophobic coatings on a cover-glass. The superhydrophobic surface on a cover-glass was prepared using a silica particulate solution previously developed by our research team.[30] In the preparation, tetraethylorthosilicate (TEOS, 5 mL) and tridecafluorooctyl triethoxysilane (FAS, 1 mL) were dissolved in 25 mL of ethanol. The solution was combined with an ammonium hydroxide/ethanol solution (6 mL of 28% $NH_3 \cdot H_2O$ in 25 mL of ethanol), and stirred intensively at room temperature for 12 hours. The prepared colloidal suspension contains silica nanoparticles ($(CH_2)_2(CF_2)_5CF_3$) between *ca.* 50 and 150 nm. The milky mixture was then subjected to 30 minutes of ultrasonic treatment (VCX750 Sonics & Materials Inc.). To prepare the superhydrophobic surface on the cover-glass, a clean cover-glass slip was completely dipped in the synthesized coating solution, followed by drying at room temperature. After curing at 110 °C for 1 h, the coated glass was ready for further use. The water contact angle (WCA) of these surfaces was measured utilizing a contact angle meter (KSV CAM101 Instruments Ltd) typically in the range of 170–176°.

(b) Ionic liquid synthesis preparation. Equimolar amounts of anhydrous trifluoromethanesulfonic acid were added drop wise to triethylamine. The neutralization reaction was carried out by cooling the amine solution to −78 °C using an acetone/dry-ice bath. The mixture was stirred at room temperature for several hours. The mixture was then vacuum dried for 24 h at 60 °C.

(c) Quantum-dot doped microdroplet solution preparation. A solution of glycerol and Milli-Q was combined in a 10/90 ratio

(v/v) and vortexed. Once the solution became homogeneous, an aliquot of 50–100 μL of water soluble CdSe/ZnS core–shells was mixed with the solution and vortexed for 1–2 minutes. Finally the solution was transferred to a fragrance atomizer for micro-droplet generation. The aliquot of QDs was typically combined with a 10 mL volume of the glycerol/water solution which resulted in a final QD concentration of 0.05–0.1 μM in the microdroplets. The QD-doped ionic liquid solution was prepared using a 50/50, v/v volumetric ratio and the QD volume as utilized above, then vortexed for 2 minutes. Spray deposition routinely produced glycerol/water and ionic liquid/water droplets on the superhydrophobic coating of typical D 5–15 μm. According to Kiraz *et al.*,[31] the glycerol/water microdroplets quickly reach a size equilibrium caused by rapid water evaporation (90% glycerol final microdroplet composition). In effect the ionic liquid microdroplets exhibit a similar outcome.

(d) Mathematical modeling of whispering gallery mode spectra and particle analysis. The particle diameter was first approximated from confocal fluorescence intensity images using the ImageJ software.[32] Specifically a 7 point smoothing analysis was completed at angular positions 0°, 45°, 90° and 135° about the particle periphery to determine the intensity cut-off region (*i.e.* visual microdroplet diameter). This analysis provides a strict lower bound to the droplet's diameter: for the droplet whose spectrum is shown in Fig. 4 this value is 8280 ± 130 μm. Spectral profiles and the droplet diameter were finally characterized with a WGM fitting routine based on Mie theory.[33] The routine is based on the formulation of Probert-Jones[34] and adds full analytic derivatives to a prior code developed by the Bieske group.[35,36] The approximate formulae of Lam *et al.*, are used for bracketing of roots.[37] The index of refraction (real part) of a 90/10 glycerol/water solution (20 °C) is given by the relation $n = 1.447 + 3970\lambda^{-2}$ by fitting to data for glycerol and water given in the literature.[31,38] Barnes *et al.*[39] demonstrate that for their nominal 7.0 μm glycerol droplets, WGMs of radial mode order 2 dominate the spectrum. The final assignments shown in Fig. 5 were made by adjusting the angular mode numbers of a sequence of TE and TM peaks while minimizing the deviation in calculated peak positions by varying the microdroplet radius and the index of refraction parameters.

Results and discussion

Overview

In Fig. 1a, high-resolution SEM micrographs of the silica coated surfaces are presented. The hydrophobicity of the coated cover-glass was then determined using a WCA tester. The photograph in Fig. 1b shows a water droplet on the superhydrophobic surface with a measured contact angle of 170 ± 2°. The very high contact angles are due to the combination of high coating porosity and the perfluorinated alkane surface chemistry. A typical emission spectrum of a QD-doped droplet (Q-factor 4.0×10^3) is presented in Fig. 1c, together with a typical emission signal acquired from a control droplet (no QDs; D 6.75 μm), which demonstrates the absence of background luminescence with our detection system. Fig. 1d shows fluorescence images of droplets doped with red, orange and green QDs.

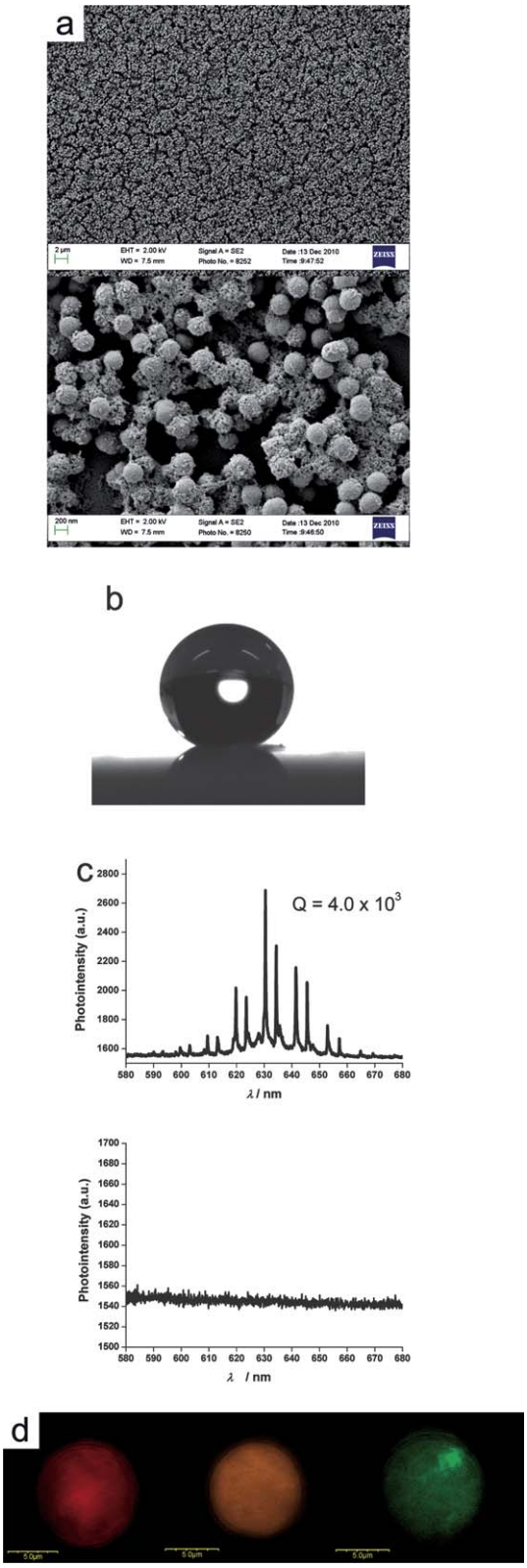

Fig. 1 Superhydrophobic coating characterization. From top of panel (a) low and high resolution SEM images of superhydrophobic coated cover-glass; (b) image of a water droplet on the fluorinated silica surface; (c) typical emission spectrum from a QD-doped microdroplet and the emission from an un-doped microdroplet and (d) typical fluorescence images of microdroplets doped with red, orange and green QDs.

Position sensitive mode coupling

The confocal system enables selection of the excitation point to a spatial resolution of 0.3 μm which is 30 times smaller than the typical droplet diameter. Excitation point selectivity was then utilized to explore the emission response at various selected points at the circumference of a droplet (Fig. 2) and determine an optimal WGM illumination position. A reference droplet transmission image indicates the selected excitation positions assigned about the droplet periphery at 0°, 45°, 90°, 135°, 180°, 225°, 270° and 315° (Fig. 2a). Emission data were collected at each assigned position using the maximum-excitation energy with a 2 s integration time (Fig. 2b). The example shows a large spectral variation in the shape and profile of each collected emission signal. While the variables that control this result were not clearly understood, the follow-up experiments utilized a fixed 0° excitation position for microdroplet excitation to minimize the variability and maximize the WGM acquisition quality.

Photostability tests

The WGM stability was measured under continuous excitation (>15 min) Fig. 3. A single microdroplet was exposed to continuous excitation (laser beam power 100%, 465.5 μW) for 20 minutes. The droplet exposure time (20 min) was selected to demonstrate an extended period of droplet illumination compared to excitation periods used with dye based systems (<2 s). All the initial WGM peaks could still be identified and did not shift significantly following photolysis. These results show

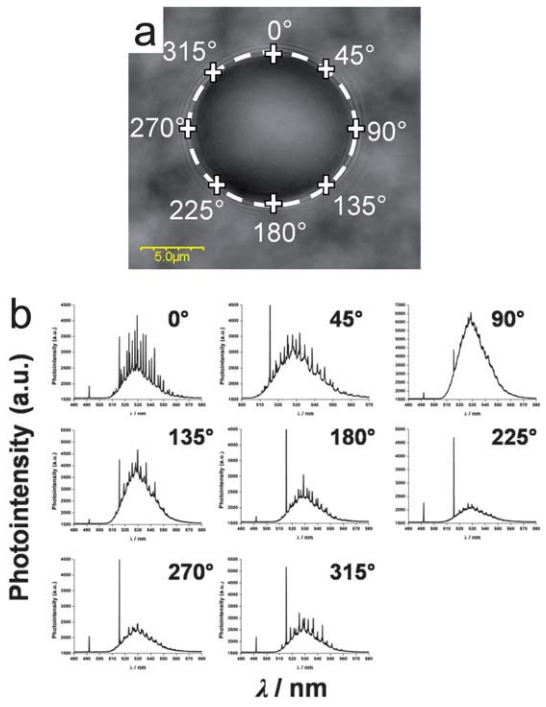

Fig. 2 Position dependent spectroscopic analysis. (a) Schematic of selected laser beam excitation positions relative to microdroplet transmission image; a droplet was excited at angular labeled positions (+) 0°, 45°, 90°, 135°, 180°, 225°, 270° and 315° about the boundary of the particle (white dashed line); (b) 7.53 μm droplet doped with 522 nm green emitting QDs.

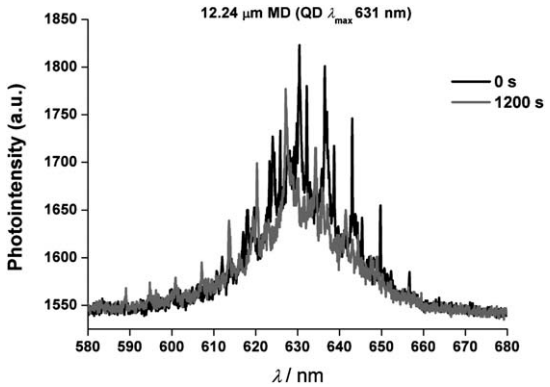

Fig. 3 WGM reporting performance. A 12.24 μm droplet was continuously excited (laser output energy 465.5 μW) and emission spectra were collected at 0 s, 300 s, 600 s, 900 s and 1200 s (ESI†); spectral overlay emission response plot of WGM emission acquired at time 0 s (black spectrum) and 1200 s (grey spectrum).

prolonged excitation of the microdroplet under extreme laser energy does not compromise WGM emission intensity and shape information.

Broad spectral range afforded by QDs

To illustrate the droplet WGM tunability, microdroplets doped with various combinations of emitting QDs were investigated. In Fig. 4 the spectrum acquired from a microdroplet doped with a mixture of QDs, green (λ_{max} 522 nm), yellow (λ_{max} 572 nm), orange (λ_{max} 615 nm) and red emitting (λ_{max} 631 nm) QDs is presented. For the selected 8.46 μm droplet more than 40 fluorescent modes are identifiable.

Detailed characterization of WGM yields size information

Theoretical characterization of WGM response curves was carried out in order to determine an accurate microdroplet diameter and index of refraction. Fig. 5 shows a portion of the spectrum of Fig. 4 between the wavelengths of 555 and 595 nm. The fitting procedure described above yielded best fit parameters for the diameter and index of refraction of the microdroplet with the assignments indicated for the nine selected WGMs. All labeled modes are of radial order 2 and have angular mode numbers from 57 to 53. Table 1 compares the experimental

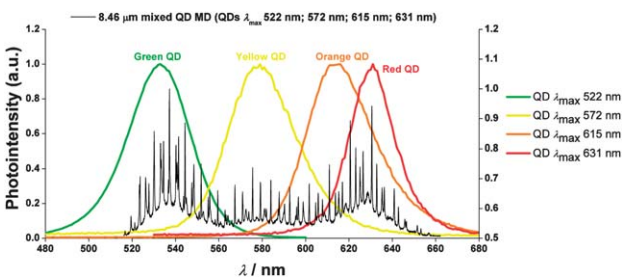

Fig. 4 Emission response acquired from a single microdroplet (D 8.46 μm) doped with a mixture of QD samples (λ_{max} 522 nm, λ_{max} 572 nm, λ_{max} 615 nm and λ_{max} 631 nm). The corresponding fluorescence emission envelopes for each QD set are overlaid.

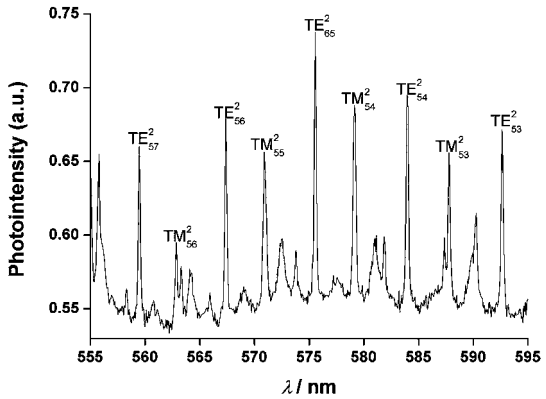

Fig. 5 Theoretical WGM emission characterization. Selected modes from the spectrum Fig. 4 are labeled for the spectral range between 559 and 595 nm.

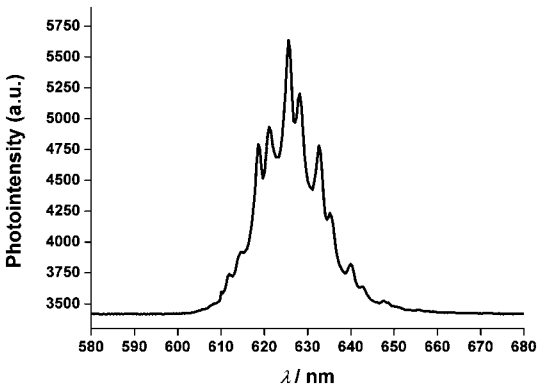

Fig. 6 Ionic liquid resonator. Typical QD (λ_{max} 622 nm) doped ionic liquid droplet emission response generated on the superhydrophobic interface.

$\lambda(\lambda_{exp})$ and calculated $\lambda(\lambda_{calc})$ positions for the 8.46 μm droplet. An absolute average deviation value of 0.095 nm and the maximum deviation 0.25 nm were calculated for the 9 lines utilized in the fit. Best fit parameters yield the droplet diameter = 8.456 μm and the index of refraction, $n = 1.365 + 29292\ \lambda^{-2}$. This derived diameter is larger than the lower bound found from visual analysis and the index of refraction is reasonably consistent with the literature value given in the Methods section (d) above. Note that the average index of refraction over the spectral range in the fit is $n = 1.453$ which corresponds to a glycerol composition of 85.4% by volume.

Ionic liquid microdroplets

Glycerol/water microdroplets support high-Q WGM emission in air, however droplet instability due to evaporation (ESI†) still presents a limitation. To obviate this difficulty, ionic liquid microdroplets were also investigated (*i.e.* without altering the platform). Ionic liquids are non-volatile solvents well known for their stability at room temperature, recyclability and tunability (*i.e.* refractive index, viscosity).[40–42] In addition ionic liquids support fluorescence emission of excited water stabilized CdSe/ZnS QDs (λ_{max} 622 nm) and are also reported to improve QD emission properties.[43,44] Fig. 6 presents a typical WGM signal generated from an immobilized single QD-doped ionic liquid microdroplet. Preliminary results have shown that QD-doped ionic liquid droplets exhibit a significant improvement in WGM blue-shift following continuous beam excitation in air (t = 20 min) compared with glycerol–water droplets (ESI†). A wide range of solutes including proteins and oligonucleotides dissolve in ionic liquids, and these data suggest ionic liquids may be an ideal platform for long term droplet studies of WGMs.

Table 1 Experimental and calculated peak maxima are compared for the WGMs labeled in Fig. 5. An absolute average deviation is 0.095 nm and the maximum deviation is 0.25 nm. Best fit parameters yield the microdroplet diameter = 8.456 μm and the average index of refraction over this spectral range, $n = 1.453$

λ_{exp}	Mode assignment	λ_{calc}	$\lambda_{calc} - \lambda_{exp}$
559.46	TE_{57}^2	559.60	0.13
562.85	TM_{56}^2	562.78	−0.06
567.38	TM_{56}^2	567.42	0.04
570.90	TM_{55}^2	570.77	−0.12
575.56	TM_{55}^2	575.52	−0.04
579.14	TM_{54}^2	579.04	−0.09
583.93	TM_{54}^2	583.89	−0.04
587.36	TM_{53}^2	587.61	0.25
592.64	TM_{53}^2	592.57	−0.07

Conclusions

Spray deposition of QD doped microdroplets produces close-to-spherical liquid drops exhibiting whispering gallery modes with Q-factors up to 4.0×10^3.

Simulated spectra using Mie theory were in good agreement with experiment. Microdroplets composed of QD doped ionic liquids were found to exhibit even longer spectral stability, due to reduced evaporation rates irrespective of QD reporter concentration. Size estimation of more than 100 lased microdroplets suggests the typical droplet diameter which supports high Q WGM emission is 9.65 μm. The high sensitivity of the WGM spectra to small changes in refractive index and temperature provides a general pathway for studying chemical reactions in microspaces.

Acknowledgements

Edin Nuhiji thanks Dr Alison Funston of Monash University, Australia for her invaluable microscope support and participation in countless enlightening scientific discussions. François G. Amar thanks Evan Bieske and Phil Wearne for introducing him to WGMs and Sam Hess for a useful discussion.

Notes and references

1 Y. P. Rakovich and J. F. Donegan, *Semicond. Sci. Technol.*, 2007, **22**, 145–148.
2 E. Nuhiji and P. Mulvaney, *Small*, 2007, **3**, 1408–1414.
3 A. M. Armani, R. P. Kulkarni, S. E. Fraser, R. C. Flagan and K. J. Vahala, *Science*, 2007, **317**, 783–787.
4 K. J. Vahala, *Nature*, 2003, **424**, 839–846.
5 E. Nuhiji and P. Mulvaney, *Nat. Mater.*, 2007, **6**, 546.
6 I. Shestopalov, J. D. Tice and R. F. Ismagilov, *Lab Chip*, 2004, **4**, 316–321.

7 S. L. Poe, M. A. Cummings, M. P. Haaf and T. D. McQuade, *Angew. Chem.*, 2006, **118**, 1574–1578.
8 H. Song and R. F. Ismagilov, *J. Am. Chem. Soc.*, 2003, **125**, 14613–14619.
9 A. Huebner, L. F. Olguin, D. Bratton, G. Whyte, W. T. S. Huck, A. J. de Mello, J. B. Edel, C. Abell and F. Hollfelder, *Anal. Chem.*, 2008, **80**, 3890–3896.
10 F. Courtois, L. F. Olguin, G. Whyte, D. Bratton, W. T. S. Huck, C. Abell and F. Hollfelder, *ChemBioChem*, 2008, **9**, 439–446.
11 J. M. Hartings, J. L. Cheung and R. K. Chang, *Appl. Opt.*, 1998, **37**, 3306–3310.
12 K. Mølhave, A. Kristensen and N. A. Mortensen, in *Advanced Photonic Structures for Biological and Chemical Detection*, ed. X. Fan, Springer, New York, 2009, pp. 471–486.
13 S. Holler, N. L. Goddard and S. Arnold, *J. Chem. Phys.*, 1998, **108**, 6545–6547.
14 A. Kiraz, M. A. Dundar, A. L. Demirel, S. Doganay, A. Kurt, A. Sennaroglu and M. Y. Yuce, *J. Nanophotonics*, 2007, **1**, 011655.
15 A. Kiraz, A. Sennaroglu, S. Doganay, M. A. Dundar, A. Kurt, H. Kalaycioglu and A. L. Demirel, *Opt. Commun.*, 2007, **276**, 145–148.
16 E. Ying, D. Li, S. Guo, S. Dong and J. Wang, *PLoS One*, 2008, **3**, e2222.
17 W. C. Chan and S. Nie, *Science*, 1998, **281**, 2016–2018.
18 A. M. Derfus, W. C. W. Chan and S. N. Bhatia, *Adv. Mater.*, 2004, **16**, 961.
19 G. Guo, W. Liu, J. Liang, Z. He, H. Xu and X. Yang, *Mater. Lett.*, 2007, **61**, 1641–1644.
20 U. Resch-Genger, M. Grabolle, S. Cavaliere-Jaricot, R. Nitschke and T. Nann, *Nat. Methods*, 2008, **5**, 763–775.
21 M. Bruchez, M. Moronne, P. Gin, S. Weiss and A. P. Alivisatos, *Science*, 1998, **281**, 2013–2016.
22 J. Pacifico, J. Jasieniak, D. E. Gómez and P. Mulvaney, *Small*, 2006, **2**, 199–203.
23 D. E. Gomez, I. Pastoriza-Santos and P. Mulvaney, *Small*, 2005, **1**, 238–241.
24 P. T. Snee, Y. H. Chan, D. G. Nocera and M. G. Bawendi, *Adv. Mater.*, 2005, **17**, 1131–1136.
25 J. Schäfer, J. P. Mondia, R. Sharma, Z. H. Lu, A. S. Susha, A. L. Rogach and L. J. Wang, *Nano Lett.*, 2008, **8**, 1709–1712.
26 J. van Embden and P. Mulvaney, *Langmuir*, 2005, **21**, 10226–10233.
27 J. Jasieniak and P. Mulvaney, *J. Am. Chem. Soc.*, 2007, **129**, 2841–2848.
28 J. van Embden, J. Jasieniak, D. E. Gómez, P. Mulvaney and M. Giersig, *Aust. J. Chem.*, 2007, **60**, 457–471.
29 E. E. Lees, T. L. Nguyen, A. H. A. Clayton and P. Mulvaney, *ACS Nano*, 2009, **3**, 1121–1128.
30 H. Wang, J. Fang, T. Cheng, J. Ding, L. Qu, L. Dai, X. Wang and T. Lin, *Chem. Commun.*, 2008, 877–879.
31 A. Kiraz, S. Doganay, A. Kurt and A. L. Demirel, *Chem. Phys. Lett.*, 2007, **444**, 181–185.
32 W. S. Rasband, US National Institutes of Health, 1997–2009, http://rsb.info.nih.gov/ij/.
33 G. Mie, *Ann. Phys.*, 1908, **25**, 377–445.
34 J. R. Probert-Jones, *J. Opt. Soc. Am. A*, 1984, **1**, 822–830.
35 A. J. Trevitt, P. J. Wearne and E. J. Bieske, *J. Aerosol Sci.*, 2009, **40**, 431–438.
36 A. J. Trevitt, P. J. Wearne, E. J. Bieske and M. D. Schuder, *Opt. Lett.*, 2006, **31**, 2211–2213.
37 C. C. Lam, P. T. Leung and K. Young, *J. Opt. Soc. Am. B*, 1992, **9**, 1585–1592.
38 D. E. Gray, *American Institute of Physics Handbook*, McGraw-Hill, New York, 1972.
39 M. D. Barnes, N. Lermer, W. B. Whitten and J. M. Ramsey, *Rev. Sci. Instrum.*, 1997, **68**, 2287.
40 M. L. Dietz and J. A. Dzielawa, *Chem. Commun.*, 2001, 2124–2125.
41 C. A. Angell, N. Byrne and J.-P. Belieres, *Acc. Chem. Res.*, 2007, **40**, 1228–1236.
42 B. Hasse, J. Lehmann, D. Assenbaum, P. Wasserscheid, A. Leipertz and A. P. Fröba, *J. Chem. Eng. Data*, 2009, **54**, 2576–2583.
43 W. Caroline and O. C. Richard, *Nanotechnology*, 2007, **18**, 025402.
44 T. Nakashima and T. Kawai, *Chem. Commun.*, 2005, 1643–1645.

